

ANALYSIS OF LOW FREQUENCY OSCILLATIONS IN ISLANDED OPERATION OF MICROGRID

Mohan MUNIAPPAN¹

Recently, the low frequency oscillation has been increased in the Microgrid since the inverter is supplying to the loads in an islanded condition due to the opening action of utility breaker. The low frequency oscillations can be seen in the voltage and current waveforms when there is a mismatch between the inverter supplying power and loads. Under the condition of low frequency oscillation, the ratio of voltage and current harmonics at the fundamental frequency \pm oscillation frequency is equal to the impedance of the actual circuit in the Microgrid. In this paper, the simulation study of low frequency oscillation is performed in an islanded operation of microgrid. In such condition, the utility breaker is disconnected the grid supply and inverter only supplying to RL loads considering power mismatch conditions. The analytical study of the impedance calculation for the actual distribution circuit is performed and that is verified with the simulation results.

Keywords: Inverter, Islanded operation, Low frequency oscillation, Microgrid

1. Introduction

In recent years, microgrid has been developed for the integration of renewable energy sources and to provide support for the local loads in the distribution systems. Due to the introduction of renewable energy sources such as wind, solar and battery energy storage systems, the power electronic converters and/or inverters are used for the power conversion [1] – [3]. Normally, In the microgrid system, the inverter-based sources are supplied to the local load and it is connected to the grid via short lines. If there is a need for isolation of grid from the inverter-based sources by opening the utility breaker, then there will be an islanding operation, i.e., inverter only supplies to the local load [4]. Under this scenario, if there is a power mismatch between the inverter-based sources and local load, then the low frequency oscillation is produced in the voltage and current responses.

In references [5] – [15], the simulation study of low frequency oscillation is carried out in the inverter interfaced power networks. However, the low frequency oscillation study is not carried out with the numerical impedance calculation and verification. During the low frequency oscillation period, the

¹ Senior Research Specialist, ALSET Lab, Rensselaer Polytechnic Institute (RPI), Troy, New York, e-mail: mohanbe.m@gmail.com

impedance of the actual distribution circuit should be equal to the ratio of voltage and current harmonics at the fundamental frequency \pm oscillation frequency. In this paper, the low frequency oscillation study is carried out in the inverter islanding operation of Microgrid by comparing the impedance of actual distribution circuit with the ratio of voltage and current harmonics at the fundamental frequency \pm oscillation frequency.

This paper is constructed as follows: Section 2 presents the low frequency oscillation scenario in the microgrid. Section 3 presents the analytical study of the impedance calculation for the microgrid system when the utility breaker is opened. Also, it presents the magnitude and phase of the impedance plot for the microgrid system. Section 4 presents the simulation of FFT analysis and calculation of ratio of voltage and current harmonics of the fundamental \pm low frequency frequencies. Section 5 presents the impedance table comparison between the analytical impedance calculation of the distribution equivalent circuit and ratio of voltage and current harmonics. Finally, section 6 concludes with the summary of important points.

2. Low Frequency Oscillation in Microgrid

The microgrid test system considered for the study is shown in Fig. 1. In this system, the 13.2 kV grid is connected to the short transmission line through the source impedance that is the combination of resistance and reactance in series and in parallel with the resistance (R_p). Then, the short line is connected to the shunt capacitors, parallel connected RL load and series connected transmission lines (Line-1 and Line-2). Finally, the transmission lines are connected to the 1 MW inverter.

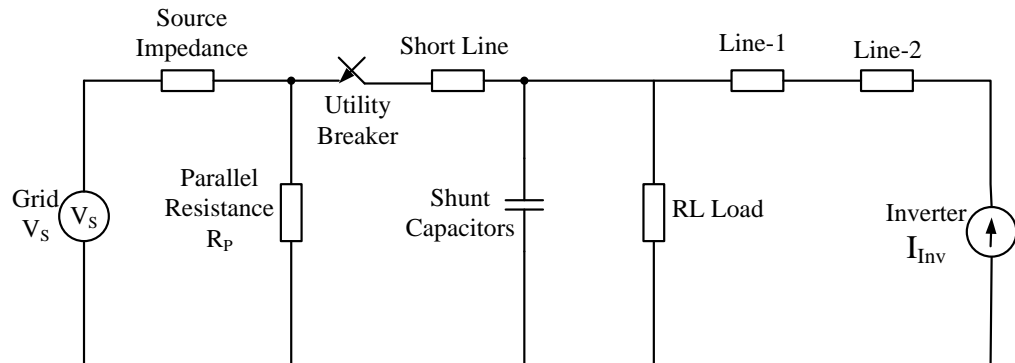


Fig. 1. Microgrid Test System.

Consider Fig. 1, when utility breaker open, the grid is disconnected from the distribution circuit. Under this condition, the inverter only supplying to the

distribution loads, i.e., RL load. If there is a mismatch occur between the power generation (i.e., inverter power) and loads (i.e., RL load), the low frequency oscillations are produced. This low frequency oscillation is continued until the utility breaker is closed, i.e., grid supply is connected back.

In this paper, the low frequency oscillation cases are presented under the condition of power mismatch condition. The power mismatch consideration is: the inverter power is considered as 1.6 MW and the RL load as 1 MW and 600 kVAR. During the low frequency oscillation, the oscillation frequency is combined with the fundamental frequency ($f_{\text{fundamental}} + f_{\text{oscillation}}$ and $f_{\text{fundamental}} - f_{\text{oscillation}}$). In such condition, the ratio of voltage and current harmonics of these two frequencies are following the impedance of the distribution circuit. If the fundamental frequency is 60 Hz and oscillation frequency is 4 Hz, then the ratio of voltage and current harmonics for 56 Hz and 64 Hz will matches the impedance of the distribution circuit.

3. Impedance of Distribution Circuit When Utility Breaker Open

In this section, the analytical study of the impedance for the actual distribution circuit is performed when the utility breaker is open. The equivalent circuit of the microgrid system when utility breaker open is shown in Fig. 2. The simplified equivalent circuit model of the system is shown in Fig. 3.

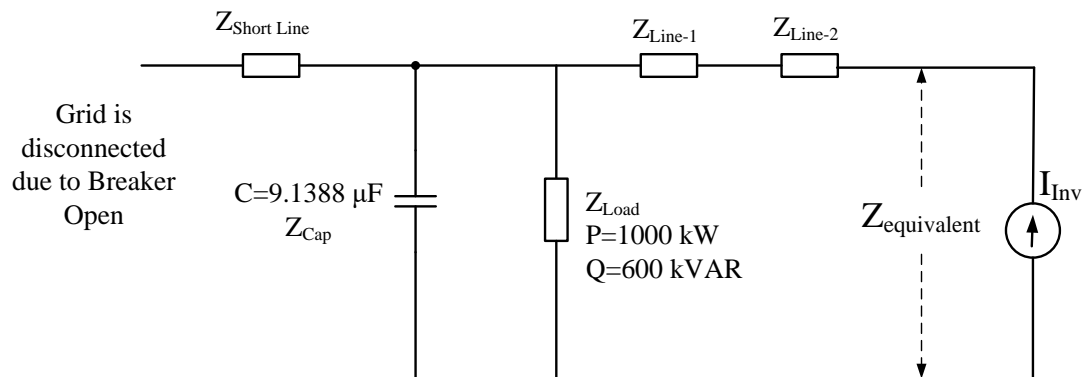


Fig. 2. Distribution circuit when utility breaker open.

3.1 Parameters of the System

Inverter power $P_{\text{Inv}} = 1600 \text{ kW}$

Load Impedance for $P = 1000 \text{ kW}$ and $Q = 600 \text{ kVAR}$

Line voltage, $V_{\text{LL}} = 13.2 \text{ kV}$, Phase voltage $V_{\text{Ph}} = 7.621 \text{ kV} = 7621 \text{ V}$

The active power load, $P = 1000 \text{ kW}$

Inductive reactive load, $Q_L = 600 \text{ kVAR}$; $Q_{L-1\text{-phase}} = 200 \text{ kVAR}$

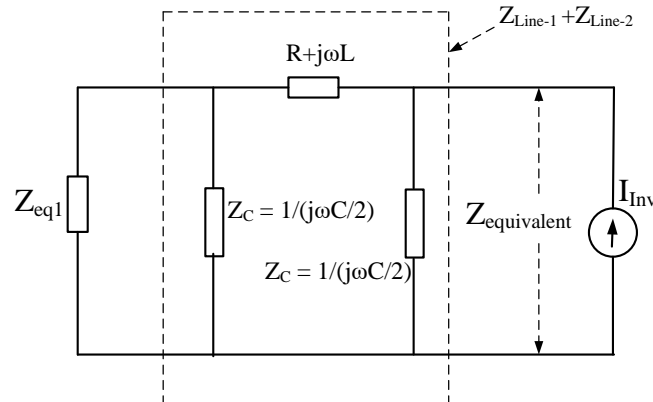


Fig. 3. Simplified equivalent circuit model.

Apparent power, $S = 1000+j600 = 1166.19 \angle 30.96^\circ \text{ kVA}$

For single phase, $S_{1\text{-phase}} = S/3 = 388.73 \angle 30.96^\circ \text{ kVA}$

Current, $I = S_{1\text{-phase}}/V_{\text{Ph}} = 51 \text{ A}$

Resistance, $R = P/(3 \times I^2) = 128.15 \Omega$

Inductive Reactance, $X_L = Q_{L-1\text{-phase}}/(I^2) = 76.89 \Omega$

Load impedance, $Z_L = (128.15+j76.89) = 149.44 \angle 30.96^\circ \Omega$

Shunt capacitor, $C = 9.1388 \mu\text{F}$

Two transmission line length is 3.26 km ($Z_{\text{Line1}} = 1.63 \text{ km} + Z_{\text{Line2}} = 1.63 \text{ km}$)

3.2 Impedance Calculation for 56 Hz

Load impedance, $Z_L = (128.15+j71.7427) = 146.86 \angle 29.24^\circ \Omega$

Impedance from shunt capacitor, $Z_{\text{cap}} = -j311.14 \Omega$

The shunt capacitor and RL load are connected in parallel, so it can be simplified as,

$$Z_{\text{eq1}} = (Z_{\text{Cap}} \times Z_L) / (Z_{\text{Cap}} + Z_L) = 168.28 \angle 1.07^\circ = (168.25+j3.14) \Omega$$

The equivalent impedance of the system is calculated by,

$$\begin{aligned} Z_{\text{equivalent}} &= Z_{\text{eq1}} + Z_{\text{Line1}} + Z_{\text{Line2}} \\ Z_{\text{equivalent}} &= 169.24 \angle -8.08^\circ = (167.55-j23.78) \Omega \end{aligned} \quad (1)$$

3.3 Impedance Calculation for 64 Hz

Load impedance, $Z_L = (128.15+j81.99) = 152.13 \angle 32.61^\circ \Omega$

Impedance from shunt capacitor, $Z_{\text{cap}} = -j272.25 \Omega$

The shunt capacitor and RL load are connected in parallel, so it can be simplified as,

$$Z_{\text{eq1}} = (Z_{\text{Cap}} \times Z_L) / (Z_{\text{Cap}} + Z_L) = 180.55 \angle -1.36^\circ = (180.49-j4.28) \Omega$$

The equivalent impedance of the system is calculated by,

$$\begin{aligned}
 Z_{\text{equivalent}} &= Z_{\text{eq1}} + Z_{\text{Line1}} + Z_{\text{Line2}} \\
 Z_{\text{equivalent}} &= 180.24 \angle -5.18^\circ = (179.50 - j16.27) \Omega
 \end{aligned} \tag{2}$$

The equivalent impedance circuit given in Fig. 2 is simulated in MATLAB and the magnitude and phase of the impedance plotted. Fig. 4 shows the magnitude and phase of impedance for the equivalent circuit of distribution system measured at the inverter terminal when the utility breaker is open. The calculated impedance for 56 Hz and 64 Hz given in equation (1) and (2) are almost similar with the impedance shown in Fig. 4.

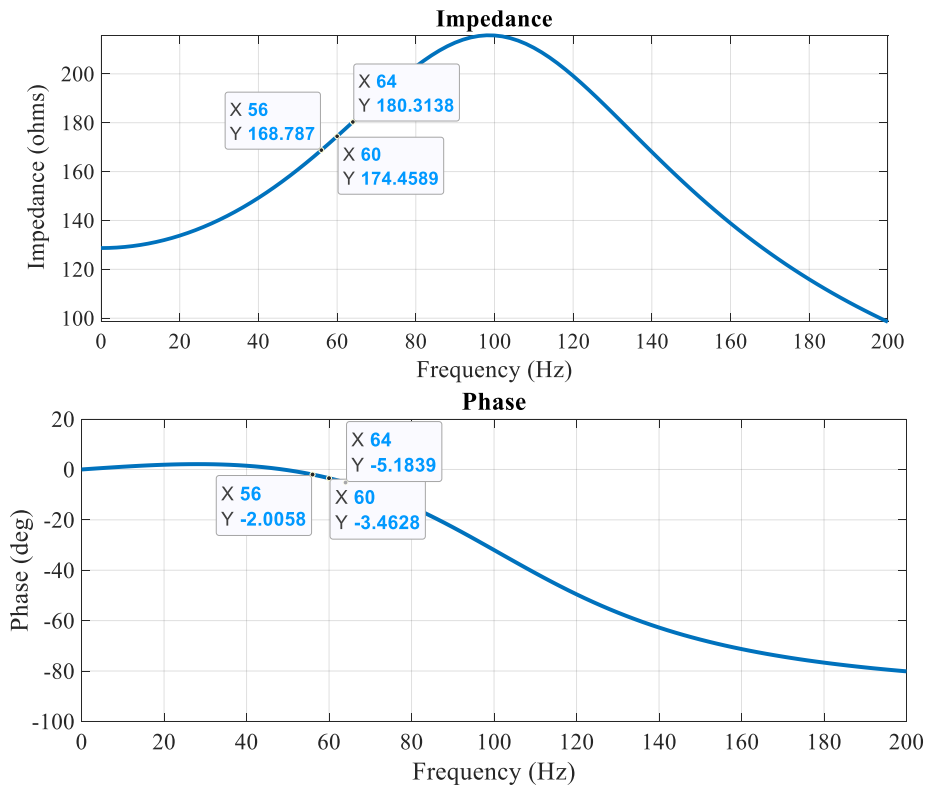


Fig. 4. Impedance plot for the equivalent circuit of distribution system at the inverter terminal when utility breaker open.

4. Ratio of Voltage and Current Harmonics Calculation

The simulation analysis is performed for the inverter power is 1.6 MW and the RL load is 1 MW and 600 kVAR. The inverter voltage and current waveforms

under power mismatch conditions are shown in Fig. 5 and Fig. 6. From these waveforms, it can be seen that, the grid supply is disconnected at 200 second by opening the utility breaker and the RL load is working with inverter supply only until 200.25 second. Therefore, the low frequency oscillation portion (i.e., inverter running with RL load under power mismatch condition) is 0.25 sec (i.e., 200.0 to 200.25 sec). From the Fig. 5 and Fig. 6, it can be seen that 4 Hz oscillation produced in the inverter voltage and current waveforms. The oscillation magnitude is larger in the inverter voltage waveform and it is very less in the inverter current waveform.

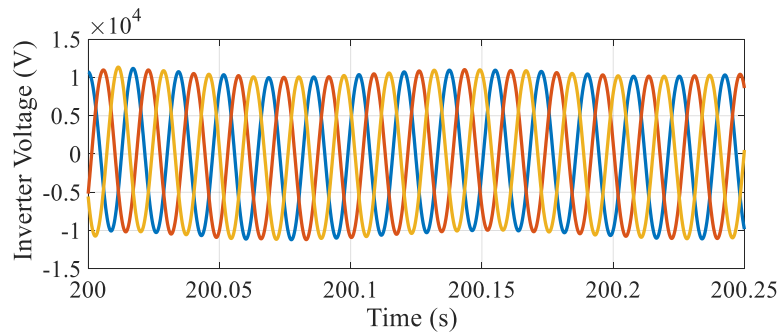


Fig. 5. Inverter voltage (V) during low-frequency oscillation period.

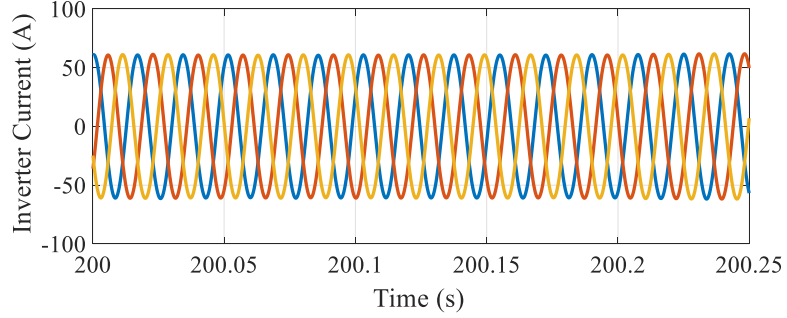


Fig. 6. Inverter current (I) during low-frequency oscillation period.

The frequency spectrum for the inverter voltage and current during low frequency portion are shown in Fig. 7 and 8. In the FFT plot, the ratio of magnitude and phase of voltage and current are calculated for each harmonic. Since the duration of the low frequency oscillation is 15 cycles (0.25 sec), the frequency resolution is 4 Hz. So, the magnitude and phase plot for voltage, current and impedance (ratio of voltage and current) are shown for every 4 Hz. From these plots, it can be seen that the fundamental frequency component is added to 56 Hz because the fundamental frequency is near to the 56 Hz when compared to 60 Hz. Therefore, the harmonic magnitude of inverter voltage and current is

dominant for 56 Hz when compared to 60 Hz. The ratio of magnitude and phase of voltage and current are shown in Fig. 9.

For 56 Hz and 64 Hz, the ratio of voltage and current is given by,

$$\text{For 56 Hz, } Z = 172.6\angle 0.97^\circ = (172.57 + j2.92) \Omega$$

$$\text{For 64 Hz, } Z = 172.8\angle 1.02^\circ = (172.77 + j3.07) \Omega$$

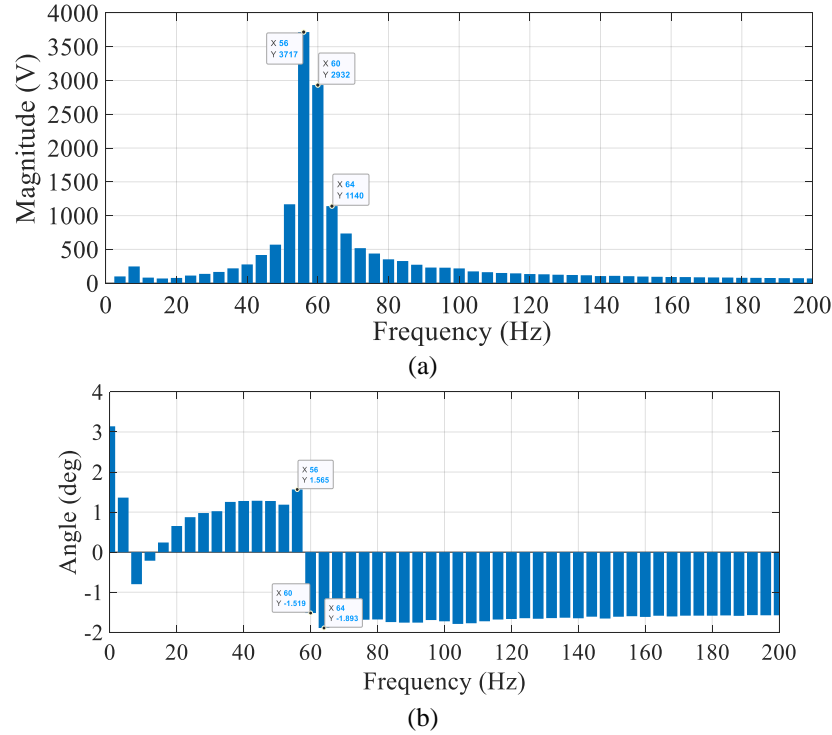
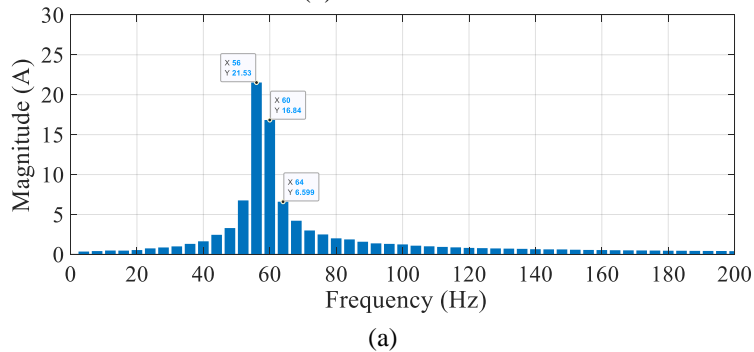
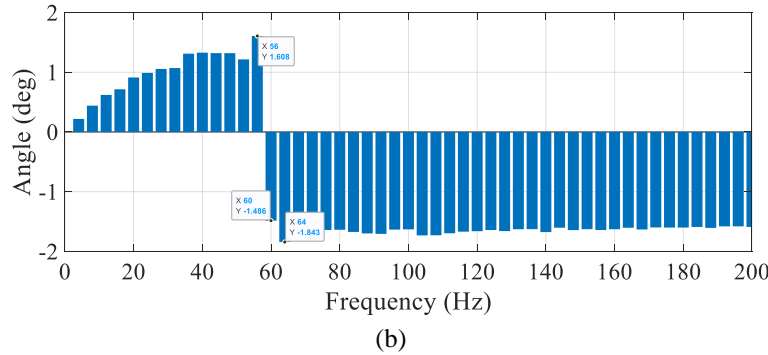


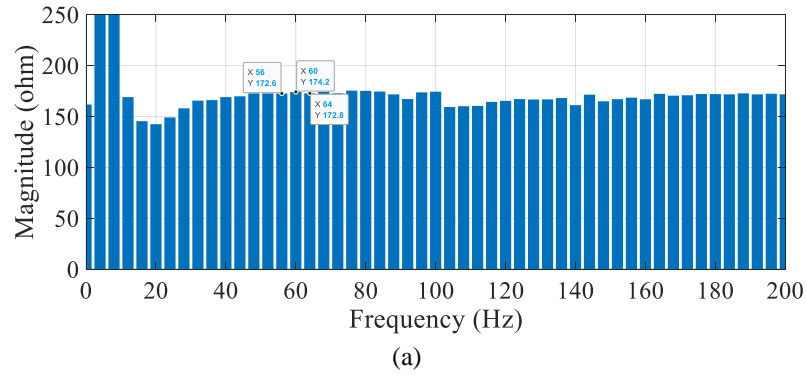
Fig. 7. FFT plot for Inverter voltage (V) for low frequency oscillation portion. (a) Magnitude of V, (b) Phase of V.



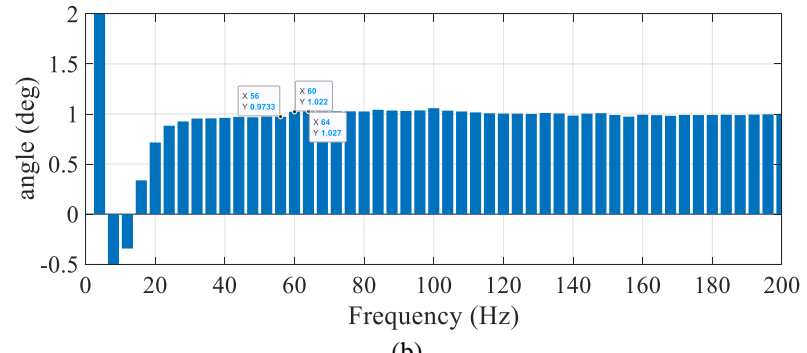


(b)

Fig. 8. FFT plot for Inverter current (I) for low frequency oscillation portion. (a) Magnitude of I, (b) Phase of I.



(a)



(b)

Fig. 9. Ratio of inverter voltage and current (V/I) for low frequency oscillation portion. (a) Magnitude of V/I, (b) Phase of V/I.

5. Impedance Table Comparison

In this section, the comparison of the impedance calculated from the actual distribution circuit and the ratio of voltage and current harmonics calculated from the FFT analysis are presented in Table 1.

Table 1
Comparing the ratio of voltage and current harmonics with the impedance calculated from the distribution circuit.

Frequency	Impedance calculation from the distribution circuit when utility breaker open	Ratio of V/I at the inverter terminal from FFT analysis
56 Hz	$169.24\angle -8.08^\circ$ (167.55-j23.78)	$172.6\angle 0.97^\circ$ (172.57+j2.92)
64 Hz	$180.24\angle -5.18^\circ$ (179.50-j16.27)	$172.8\angle 1.02^\circ$ (172.77+j3.07)

6. Conclusions

In this paper, the low frequency oscillation cases are simulated under the condition of power mismatch between the inverter power and loads. The power mismatch consideration is: the inverter power is considered as 1.6 MW and the RL load as 1 MW and 600 kVAR. During the low frequency oscillation, the oscillation frequency is combined with the fundamental frequency ($f_{\text{fundamental}} + f_{\text{oscillation}}$ and $f_{\text{fundamental}} - f_{\text{oscillation}}$). In such condition, the ratio of voltage and current harmonics of these two frequencies are equal to the impedance of the distribution circuit.

The ratio of voltage and current harmonics are calculated using Fourier analysis. Then, the impedance of the distribution circuit is calculated analytically when the utility breaker is open. Finally, the ratio of voltage and current harmonics are compared with the impedance calculated from the distribution circuit. From the table results, it can be seen that, the magnitude and phase of impedance values for both the cases are almost same. In such a way, the low frequency oscillation is verified in an islanded operation of Microgrid.

R E F E R E N C E S

- [1] Muniappan, Mohan. "A comprehensive review of DC fault protection methods in HVDC transmission systems." *Protection and Control of Modern Power Systems* 6, no. 1 (2021): 1-20.
- [2] Mohan, M., and K. Panduranga Vittal. "DC Fault Protection in Multi-terminal VSC-Based HVDC Transmission Systems with Current Limiting Reactors." *Journal of Electrical Engineering & Technology* 14, no. 1 (2019): 1-12.
- [3] Mohan, M., and K. Panduranga Vittal. "Modeling and simulation studies on performance evaluation of three-terminal VSC-HVDC link connected offshore wind farms." In *2017 International Conference on Energy, Communication, Data Analytics and Soft Computing (ICECDS)*, pp. 473-478. IEEE, 2017.
- [4] Tran, Thanh Son, Duc Tuyen Nguyen, and Goro Fujita. "The analysis of technical trend in islanding operation, harmonic distortion, stabilizing frequency, and voltage of islanded entities." *Resources* 8, no. 1 (2019): 14.

- [5] Pogaku, Nagaraju, Milan Prodanovic, and Timothy C. Green. "Modeling, analysis and testing of autonomous operation of an inverter-based microgrid." *IEEE Transactions on power electronics* 22, no. 2 (2007): 613-625.
- [6] Liu, Zeng, Jinjun Liu, Dushan Boroyevich, and Rolando Burgos. "Stability criterion of droop-controlled parallel inverters based on terminal-characteristics of individual inverters." In *2016 IEEE 8th International Power Electronics and Motion Control Conference (IPEMC-ECCE Asia)*, pp. 2958-2963. IEEE, 2016.
- [7] Wang, Yanbo. "Stability Assessment of Inverter-fed Power Systems." PhD Dissertation, Aalborg University, Denmark, (2017).
- [8] Nikolakakos, Iraklis P., Hatem H. Zeineldin, Mohamed Shawky El-Moursi, and James L. Kirtley. "Reduced-order model for inter-inverter oscillations in islanded droop-controlled microgrids." *IEEE Transactions on Smart Grid* 9, no. 5 (2017): 4953-4963.
- [9] Tao, Yong, Yan Deng, Guangdi Li, Guipeng Chen, and Xiangning He. "Evaluation and comparison of the low-frequency oscillation damping methods for the droop-controlled inverters in distributed generation systems." *Journal of Power Electronics* 16, no. 2 (2016): 731-747.
- [10] Lahiji, Houman, Jafar Mohammadi, Firouz Badrkhani Ajaei, and Ryan Boudreau. "Damping power oscillations in the inverter-dominated microgrid." In *2018 IEEE Electrical Power and Energy Conference (EPEC)*, pp. 1-7. IEEE, 2018.
- [11] Wang, Yanbo, Xiongfei Wang, Zhe Chen, and Frede Blaabjerg. "Small-signal stability analysis of inverter-fed power systems using component connection method." *IEEE Transactions on Smart Grid* 9, no. 5 (2017): 5301-5310.
- [12] Ahmed, Moudud, Lasantha Meegahapola, Arash Vahidnia, and Manoj Datta. "Analysis and mitigation of low-frequency oscillations in hybrid AC/DC microgrids with dynamic loads." *IET Generation, Transmission & Distribution* 13, no. 9 (2019): 1477-1488.
- [13] Sun, Chu, Geza Joos, and Francois Bouffard. "Identification of low-frequency oscillation mode and improved damping design for virtual synchronous machines in microgrid." *IET Generation, Transmission & Distribution* 13, no. 14 (2019): 2993-3001.
- [14] Wang, Shike, Zeng Liu, Jinjun Liu, Dushan Boroyevich, and Rolando Burgos. "Small-signal modeling and stability prediction of parallel droop-controlled inverters based on terminal characteristics of individual inverters." *IEEE Transactions on Power Electronics* 35, no. 1 (2019): 1045-1063.
- [15] Cao, Wenchao, Yiwei Ma, Fei Wang, Leon M. Tolbert, and Yaosuo Xue. "Low-frequency stability analysis of inverter-based islanded multiple-bus AC microgrids based on terminal characteristics." *IEEE Transactions on Smart Grid* 11, no. 5 (2020): 3662-3676.